Hydraulic Behavior of Collapsible Compacted Gneiss Soil

José H. F. Pereira[1]; Delwyn G. Fredlund[2]; Manoel P. Cardão Neto[3]; and Gilson de F. N. Gitirana Jr., M.ASCE[4]

Abstract: The hydraulic behavior of a residual gneiss soil compacted at conditions that produce collapsible characteristics was studied using a triaxial permeameter system that allows independent control of net stresses and matric suction. Wetting paths under differing but constant loads were utilized to reflect field conditions associated with a collapsing soil earth fill dam. The experimental results showed that different stress paths produce different amounts of volumetric collapse and distinct variations in the coefficient of permeability, which at relatively high matric suctions was mainly affected by the increase in degree of saturation. However, as the soil approached saturation, the coefficient of permeability became dependent on void ratio and net mean stress, with the saturated coefficient of permeability being reduced at larger amounts of collapse. The results also suggested that entrapped air in the soil voids may produce a significant reduction in the coefficient of permeability. A constitutive relationship for the coefficient of permeability that takes net mean stress changes into account was proposed based on best-fit analyses.

DOI: 10.1061/(ASCE)1090-0241(2005)131:10(1264)

CE Database subject headings: Unsaturated soils; Permeability; Hydraulic conductivity; Soil water; Layered soils; Constitutive models.

Introduction

Darcy's law with a variable coefficient of permeability has traditionally been used to model water flow through unsaturated soils. It is generally accepted that the coefficient for permeability of an unsaturated soil varies in response to the amount of water in the soil (Childs and Collis-George 1950). Changes in the coefficient of permeability can be interpreted as a response to changes in the cross section for water flow and changes in the flow path tortuosity. Lloret and Alonso (1980), Fredlund (1981), and Fredlund and Rahardjo (1993), among others, pointed out that the unsaturated soil coefficient of permeability may be affected by changes in both the degree of saturation and the void ratio of the soil. This is particularly true for expansive and collapsible soils that can undergo large volume changes (Huang et al. 1998a).

Extensive research can be found in the literature on the hydraulic properties of unsaturated soils (Gardner 1961; Brooks and Corey 1964; van Genuchten 1980; Mualem 1986; Fredlund et al. 1994). Most previous studies consider only the effects of water content change and focus on soils that do not exhibit significant volume change. Relatively little information is available on the hydraulic behavior of unsaturated soils such as collapsible soils, which undergo significant volume changes. Collapsible (i.e., metastable-structured) soils undergo significant and irreversible volume decrease in response to changes in the stress-state variables, such as a decrease in matric suction (Barden et al. 1973; Maswoswe 1985; Lawton et al. 1991).

The main objective of the present study was to investigate experimentally the hydraulic behavior of a residual soil of gneiss compacted at collapsible conditions. The hydraulic properties of this soil are essential to understanding the coupled hydromechanical behavior of the so-called "Alka-Seltzer" dams found in northeast Brazil (Pereira 1996). These low-cost, small dams have a typical height of about 10 m and are usually constructed of residual soil derived from gneiss (Miranda 1988). The main purpose of Alka-Seltzer dams is to store water for irrigation and public consumption throughout the long arid seasons.

Poor compaction conditions result from a lack of proper compaction equipment and compaction water. Hundreds of failures of such dams were observed during the 1990s (Miranda 1988). Typical Alka-Seltzer dams appear stable for the as-compacted conditions, but failures commonly occur shortly after the first reservoir filling (Miranda 1988; Pereira 1996; Pereira and Fredlund 1999). Field observations have indicated that the occurrence of cracks due to differential settlements and overall upstream slope failures contributed to most of the failures. Pereira (1996) and Brito et al. (2004) subsequently corroborated these field observations using theoretical models for stability analysis.

A series of triaxial permeameter tests were performed on specimens compacted at conditions reflecting the actual field conditions of the Alka-Seltzer dams. Wetting and compression paths were followed to produce a constitutive surface for the coefficient of permeability corresponding to total and water volume changes for the metastable-structured soil. A detailed description of the testing procedure is provided herein, followed by the testing pro-

[1]Associate Professor, Dept. of Civil and Environmental Engineering, Univ. of Brasília, 70910-900 Brasilia, DF, Brazil.

[2]Professor Emeritus, Dept. of Civil and Geological Engineering, Univ. of Saskatchewan, 57 Campus Dr., Saskatoon, SK, Canada S7N 5A9.

[3]Graduate Student, Dept. of Civil and Environmental Engineering, Univ. of Brasília, 70910-900 Brasilia, DF, Brazil.

[4]Graduate Student, Dept. of Civil Engineering, 57 Campus Dr., Univ. of Saskatchewan, Saskatoon, SK, Canada S7N 5A9. E-mail: gilson.gitirana@usask.ca

Note. Discussion open until March 1, 2006. Separate discussions must be submitted for individual papers. To extend the closing date by one month, a written request must be filed with the ASCE Managing Editor. The manuscript for this paper was submitted for review and possible publication on September 20, 1999; approved on October 25, 2004. This paper is part of the ***Journal of Geotechnical and Geoenvironmental Engineering***, Vol. 131, No. 10, October 1, 2005. ©ASCE, ISSN 1090-0241/2005/10-1264–1273/$25.00.

Table 1. Index Properties of Silty Sand

Index property	Data
Natural water content	2%
Typical grain-size distribution	Sand=52%, silt=35%
	Clay=13%
	D10=0.0006 mm
	D30=0.016 mm
	D60=0.22 mm
Atterberg limits	w_L=29%
	w_P=17%
	PI=12%
Specific gravity	G_s=2.64
Compaction	Standard effort
ASTM D698-91	w_{opt}=14.5%
Unified soil classification system	SM-ML

Note: Source is Pereira (1996).

gram results. The effect of changes in degree of saturation and void ratio on the hydraulic properties of the collapsible soil is analyzed. It is shown that the amount of collapse has a significant influence on the coefficient of permeability. A permeability fitting model based on the experimental results is presented.

Characterization and General Properties of Soil

The laboratory program was designed to study the mechanical behavior and hydraulic properties of a compacted gneiss soil subjected to gradual saturation (Pereira 1996; Pereira and Fredlund 2000). The tests were designed to reflect the transition from unsaturated to saturated soil conditions during the first reservoir filling of an Alka-Seltzer dam. The preliminary soil testing program consisted of compaction tests, double-oedometer tests, pressure plate tests, and Tempe cell tests. The information obtained from these preliminary tests aided in planning the testing program using the triaxial permeameter.

Characterization and Compaction Conditions

Table 1 presents the index properties of the soil studied, which is a residual silty sand derived from granitic gneiss of the Ceará group. The soil has a well-graded grain-size distribution and a small clay fraction, resulting in a plasticity index of 12%, and is representative of the soil used in the construction of so-called Alka-Seltzer dams in northeast Brazil. Miranda (1988) and Pereira (1996) used this material in the study of failure mechanisms associated with Alka-Seltzer dams during first reservoir filling.

The laboratory program presented herein focuses on defining the hydraulic properties of the residual soil compacted at dry of optimum water content conditions at a dry density lower than that obtained by using standard AASHTO energy. This compaction condition results in a metastable-structured (i.e., collapsible) soil similar to that encountered in the small dams constructed in semi-arid areas of northeast Brazil (Miranda 1988). These dams are typically constructed in an attempt to accumulate runoff water during the short rainy season, thereby providing water for the population. At least part of the original fabric of the soil has been largely destroyed since the study focuses on remolded/compacted soil.

Fig. 1 shows the compaction curve obtained using AASHTO

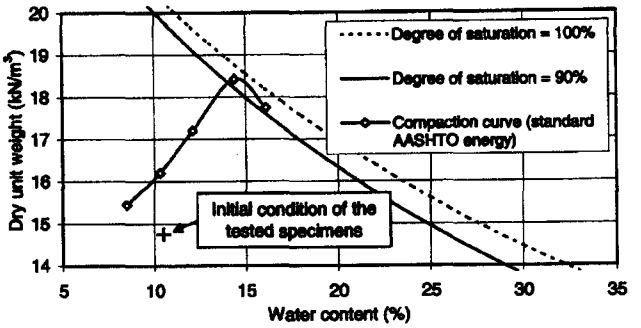

Fig. 1. Compaction curve of residual soil of gneiss

standard energy along with the compaction condition selected for specimens used in the testing program. Optimum conditions corresponding to a dry density of 18.44 kN/m^3 and water content of 14.5% produced a void ratio of 0.404. Specimens extracted from Alka-Seltzer dams show an average dry density of 14.75 kN/m^3 (Miranda 1988). The observed dry density of 14.75 kN/m^3 and a compaction water content of 10.5% were selected to reflect field conditions. Therefore, the initial conditions of the soil specimens correspond to a water content 4% dry of optimum conditions and a density about 90% of the corresponding point on the AASHTO standard compaction curve, producing a void ratio of 0.756. Miranda (1988) presented laboratory data showing the collapsible characteristics of the gneiss soil compacted at similar conditions.

Subsequent laboratory tests (i.e., double-oedometer, pressure plate, Tempe cell, and triaxial permeameter tests) were performed on statically compacted specimens using material passing the 2.0 mm sieve. The amount of material larger than 2 mm was less than 2%. This procedure was used to obtain compacted specimens of a conventional size for laboratory testing. The chosen dry density of 14.75 kN/m^3 was achieved by taking a calculated mass of soil at the selected water content (10.5%) and carefully compacting it to a calculated final volume. Double-oedometer specimens were statically compacted inside the oedometer ring, while pressure plate, Tempe cell, and triaxial permeameter specimens were statically compacted in larger molds and trimmed to the required dimensions.

Static compaction was selected for applying constant compaction energy throughout the specimens and to obtain homogeneous specimens. It was assumed that the water content and dry density (or void ratio) matching typical field conditions results in specimens with the same soil fabric and hydromechanical behavior of the soil that comprises an Alka-Seltzer dam. No attempt was made to assess the importance of eventual differences in fabric obtained using the actual field and laboratory compaction methods.

Properties of Soil Compacted Dry of Optimum Conditions

Fig. 2 presents the results of double-oedometer tests performed to determine the potential for collapse of the soil compacted at optimum and 4% dry of optimum conditions. The soil specimens were statically compacted in the oedometer ring and loaded to total vertical stresses, σ_v, ranging from 0 to 800 kPa; the vertical stresses at inundation were 25 and 400 kPa. The specimens compacted at optimum conditions showed no apparent collapsing behavior. The coefficient of compressibility of the specimen compacted at optimum conditions yielded a compression index equal

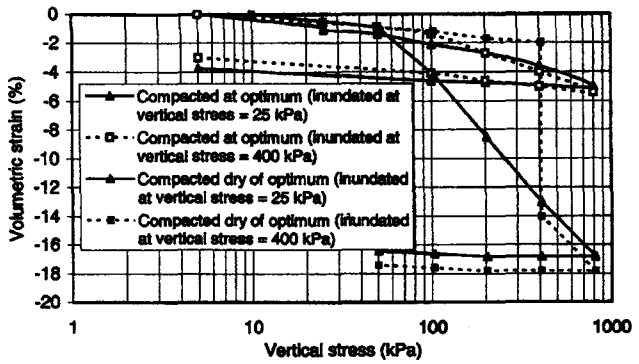

Fig. 2. Double-oedometer test on residual soil of gneiss compacted at metastable conditions

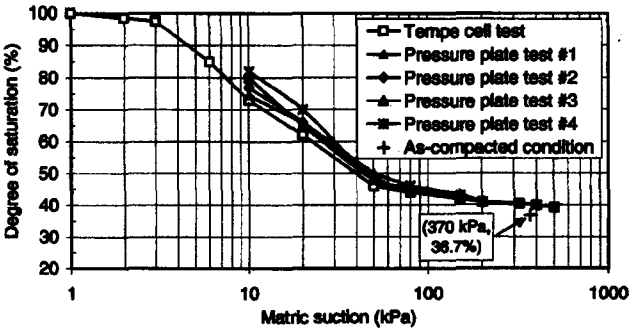

Fig. 4. Characteristic drying soil-water curve of collapsible soil

to 0.056, a value significantly lower than that of the inundated specimen compacted dry of optimum (i.e., C_c=0.242), but slightly higher than that of the unsaturated soil compacted dry of optimum (i.e., C_c=0.019). Although the symbol for compression index, C_c, has been used to represent the compressibility of the soil specimens, it is not clear whether a virgin compression curve was reached for the noninundated specimen compacted dry of optimum.

Collapse was quantified by taking the difference in volumetric strain (%) between the as-compacted and inundated specimens. The data presented in Fig. 2 show that the soil compacted dry of optimum does not suffer collapse upon inundation with a vertical stress, σ_v, lower than 50 kPa. The dry-of-optimum specimen inundated at σ_v equal to 25 kPa and loaded to σ_v equal to 100 kPa, and later to σ_v equal to 200 kPa, presented volumetric collapse values of 3.0 and 7.2%, respectively. Upon saturation by inundation at σ_v equal to 400 kPa, the measured soil collapse was greater than 11%. A similar amount of volume change was obtained for the specimen compacted dry of optimum inundated at σ_v equal to 25 kPa and loaded to σ_v equal to 400 kPa. A similar response was observed for both dry-of-optimum specimens when the vertical stresses were increased to 800 kPa. Unloading produced little volumetric strain recovery for all specimens.

Falling-head permeability tests were performed using the oedometer apparatus and the collapsing soil specimen inundated at a vertical stress of 25 kPa. The saturated coefficient of permeability was obtained for several values of vertical stress, after equilibrium was achieved for each load. Fig. 3 illustrates the results in terms of the logarithm of the saturated coefficient of permeability versus void ratio. The vertical stress corresponding to each void ratio is also indicated in the test boxes. If the fabric of the saturated soil remains constant during consolidation, a linear relationship is anticipated between the logarithm of coefficient of permeability versus void ratio (Lambe and Whitman 1979). Fig. 3 shows a slightly nonlinear variation between the logarithm of saturated coefficient of permeability and void ratio. The nonlinearity may be attributable to changes in soil fabric during collapse. The figure shows an increased nonlinearity of the curve beyond a vertical stress of 200 kPa.

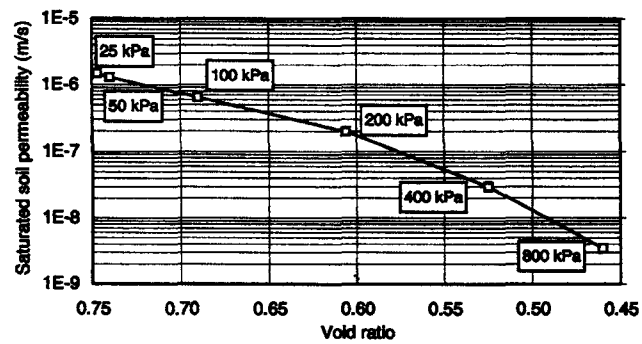

Fig. 3. Falling-head test results for saturated soil specimen at various vertical stresses (indicated in text boxes)

Fig. 4 shows the drying soil-water characteristic curve for the collapsing soil, obtained using a Tempe cell and a pressure plate apparatus in accordance with the ASTM D3152-72 designation. When using the Tempe cell test, it was possible to apply a starting matric suction of 1.0 kPa for the first matric suction step. The pressure plate tests were started at a matric suction of 10 kPa so that the soil specimens could be removed intact from the pressure chamber. The results showed an air-entry value of approximately 3.0 kPa and a residual degree of saturation of about 40%.

An initial matric suction of 370 kPa was measured on specimens compacted at a water content of 10.5% and dry density of 14.75 kN/m^3, using the null-type, axis-translation technique (Fredlund and Rahardjo 1993). The measured matric suction of 370 kPa is shown using a cross symbol (+) in Fig. 4. The value of 370 kPa corresponds to the initial suction for the specimens used in the suction-controlled triaxial permeameter tests. The as-compacted initial degree of saturation of 36.7% was never reached during the drying tests presented in Fig. 4.

The data presented in Fig. 4 were combined with the measured saturated coefficients of permeability to obtain an estimate of the change in permeability with respect to matric suction. The Brooks and Corey (1964) method was used in the interpretation of the data:

$$k_w = k_s \quad \text{for } (u_a - u_w) < (u_a - u_w)_b \tag{1}$$

$$k_w = k_s[(u_a - u_w)_b/(u_a - u_w)]^{\eta}$$
$$\text{for } (u_a - u_w) \geq (u_a - u_w)b$$

where k_w=unsaturated coefficient of permeability; k_s=the saturated coefficient of permeability; (u_a-u_w)=the matric suction; $(u_a-u_w)_b$=the air-entry value; $\eta=2+3\lambda$; $\lambda=\Delta \log S_e/\Delta \log(u_a-u_w)$; and $S_e=[(S-S_{res})/(1-S_{res})]$. The portion of the soil-water characteristic curve past the air-entry value is assumed to follow a straight line when plotted as $\log S_e$ versus $\log(u_a-u_w)$. The estimated k_w function provides an estimation of the range of matric suctions that should be used in the triaxial permeameter tests. The analysis indicates that under applied matric suctions of

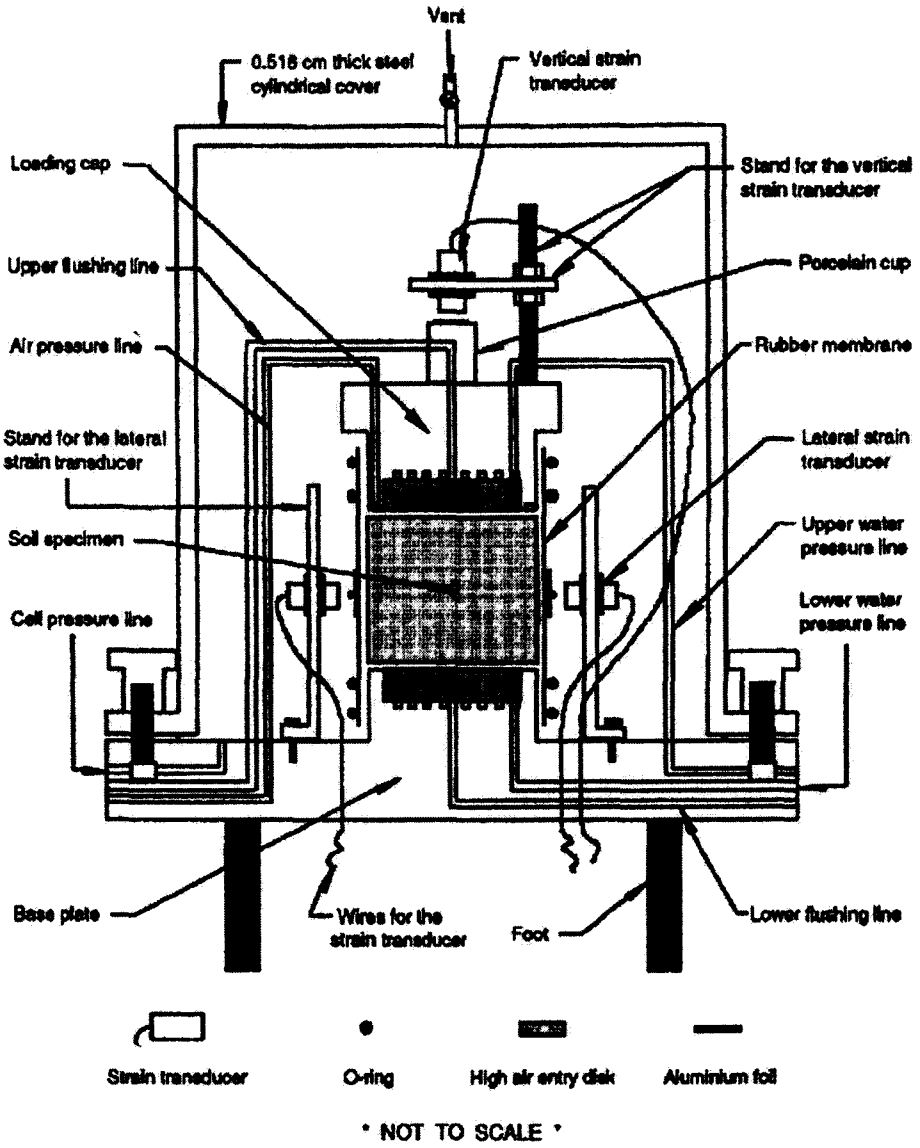

Fig. 5. Triaxial permeameter apparatus (Huang et al. 1998b) (reprinted with permission, Canadian Research Council Press)

80 and 370 kPa, the unsaturated coefficient of permeability is 1×10^{-11} and 1×10^{-13} m/s, respectively. Therefore, a much longer time would be required to attain steady-state water flow conditions in the as-compacted soil specimen (i.e., suction of 370 kPa) when compared to a specimen tested at a matric suction of 80 kPa. The time for equilibrium would also depend on the dimensions of the compacted specimen. More details about the triaxial permeameter apparatus setup and the time allowed for equilibrium during the test will be given in the following section.

Laboratory Testing Program

The coefficient of permeability and volume change for the metastable soil was measured using the triaxial permeameter apparatus developed by Huang et al. (1998b). The testing program using the triaxial permeameter was designed based on the results of the preliminary tests presented previously. This section presents a concise description of the apparatus, loading paths, and testing procedures.

Triaxial Permeameter Apparatus

Fig. 5 shows the triaxial permeameter apparatus used in this study (Huang et al. 1998b). Total stress, σ, the pore-air pressure, u_a, and the pore-water pressure, u_w, can be independently controlled, allowing the stress state within the specimen to be defined during the test. Pressure lines were controlled by pressure regulators and transferred to the water through an air/water tank. Pore-air pressures were applied at the top of the specimen, and pore-water pressures were applied at both the top and bottom, as indicated in Fig. 5. This arrangement was required to allow the application of controlled gradients of pore-water pressure. During most of the test period, equal pore-water pressures were applied at the top and bottom of the specimen. Gradients were applied only after equilibrium was reached for each pore-water pressure step. A differ-

Table 2. Stress State Paths and Equilibrium Times for Triaxial Permeameter Tests

Step	Stress-state variable (kPa)	TPT1	TPT2	TPT3	TPT4	Equilibrium time (days)
0–6	$(\sigma-u_a)$	20	50	100	200	—
0	(u_a-u_w)	370	370	370	370	1
1	(u_a-u_w)	90	—	—	90	14–24
2	(u_a-u_w)	60	60	60	60	10–14
3	(u_a-u_w)	30	30	30	30	5–10
4	(u_a-u_w)	—	—	10	10	2–4
5	(u_a-u_w)	—	—	5	5	1–2
6	(u_a-u_w)	0	0	0	0	1

ential pressure transducer manufactured by the instruments division of Bell & Howell Corporation (Huang et al. 1998b) facilitated the application of gradients measured with an accuracy of 0.015 kPa.

The inflow and outflow of water were accurately measured by using twin burettes with a volume of 10 cm^3 and a resolution of 0.02 cm^3. The outflow of water is influenced by the volume of diffused air, thereby requiring an independent measurement of diffused air. The triaxial system allows the flushing of diffused air bubbles and the measurement of the volume of the diffused air (Fredlund and Rahardjo 1993). Two flushing lines connected to the diffused air volume indicators were placed at each end of the soil specimen.

The triaxial permeameter system has the ability to measure total volume changes, and therefore the volume of the specimen was known at all stages. The deformation of the specimen was measured using a "noncontacting" displacement-measuring system (Fig. 5). Two of the noncontacting strain transducers were laterally arranged to measure changes in diameter, while the third transducer was installed to monitor the change in height of the specimen. The coefficient of permeability was obtained from these tests as a function of either the volume-mass properties or the stress-state variables.

High air-entry value ceramic disks (1 bar high flow) 10.13 mm thick were sealed into the loading cap and the base pedestal at both ends of the soil specimen. The coefficient of permeability with respect to water for the ceramic disks is approximately 8.60×10^{-8} m/s. Fredlund and Rahardjo (1993) recommend a minimum impedance factor of 10, but a factor of 1 can still produce acceptable results. The coefficient of permeability of the soil that corresponds to impedance factors of 1 and 10 are equal to $k_w=4.23\times10^{-7}$ m/s and $k_w=4.23\times10^{-8}$ m/s, respectively. A comparison between these values and the results presented in Fig. 3 indicates that the permeameter setup can be used for the measurement of coefficients of permeability to near saturation conditions.

Testing Procedure

Unsaturated and statically compacted specimens 44.8 mm high and 101.1 mm in diameter were used with the exception of test TPT1, where the specimen had a height of 54.8 mm and a diameter of 101.1 mm. Table 2 shows the stress state variables' paths applied to the soil specimens and the equilibrium times for each test stage. Four triaxial permeability tests (TPT1, TPT2, TPT3, and TPT4) were conducted on four statically compacted, collapsing soil specimens following wetting paths under a constant confining stress (net normal stress, $\sigma-u_a$). The matric suction (u_a-u_w) was reduced in steps from 370 to 0 kPa.

Measurements of the coefficient of permeability were limited to soil suctions from 0 to 90 kPa to obtain feasible testing times. The range of net normal stress values was 20 to 200 kPa, corresponding to the range of stresses commonly encountered in Alka-Seltzer dams. Similar procedures were used for the four tests. TPT1 was a pilot test used to define the testing procedures involved in assembling the soil specimen in the triaxial permeameter and monitoring volume changes. Based on the results of test TPT1, it was decided to reduce the height of the specimens in the remaining tests to reduce the equilibration time.

Each soil specimen was placed in the permeameter at its as-compacted initial condition and at an initial matric suction of 370 kPa. The specimens were isotropically loaded under a specified net normal confining pressure (Table 2). The pore-air pressure was controlled in a drained mode, and the pore-air and pore-water pressures were then adjusted to the defined initial matric suction and the specimen allowed to equilibrate. A total head gradient was then applied to the ends of the specimen for the measurement of the coefficient of permeability. The pore-water pressure differences applied were in the range of 4 to 5 kPa. A linear pore-water pressure distribution was assumed within the specimen once steady-state seepage conditions were reached. After the coefficient of permeability was measured, the matric suction imposed upon the soil specimen was reduced for the next stage while keeping the confining net normal stress constant. The procedure was repeated for several stages until the matric suction was reduced to zero.

The assessment of the equilibrium conditions involved consideration of the total and water volume change of the specimen and the water flow through the specimen. The total equilibrium time for the first stage ranged from 14 to 24 days. The equilibrium times decreased as matric suction was reduced (see the right-hand column in Table 2). Tests TPT2–4 required approximately 5 weeks to be completed, depending on the number of stages, and test TPT1 required 8 weeks for completion due to the larger soil specimen.

Air that diffused through the ceramic disks was flushed and measured every 24 h. At the end of the tests, the specimens required a back pressure of about 4 kPa to reach saturation. The triaxial system performed satisfactorily in terms of amount of leakage and volume measurements (total, water, and diffused air volume). A comparison between the total volume change of a saturated specimen and the amount of water outflow from the specimen indicated that the system of noncontact transducers provided an accurate measurement of volume changes of the specimen.

Laboratory Testing Results

Constitutive relationships were obtained for the volume change and the hydraulic behavior of the compacted, collapsing soil subjected to compression and wetting paths. The next sections present the experimental results obtained using the triaxial permeameter apparatus and the results analysis.

Volume Change Behavior of Collapsing Soil

Table 3 presents a summary of the changes in both total volume and water volume versus matric suction for the four soil specimens tested. The deformation variables were calculated using a

Table 3. Summary of Volume-Mass Properties of Specimens Tested in Triaxial Permeability Tests

Test number	TPT1	TPT2	TPT3	TPT4
Initial void ratio (e_i)	0.754	0.754	0.754	0.754
Final void ratio (e_f)	0.748	0.740	0.648	0.558
Initial water content [w_i(%)]	10.50	10.50	10.50	10.50
Final water content [w_f(%)]	27.72	26.96	24.00	21.71
Initial degree of saturation (S_i)	36.5	36.5	36.5	36.5
Final degree of saturation (S_f)	98.5	96.2	97.8	95.6

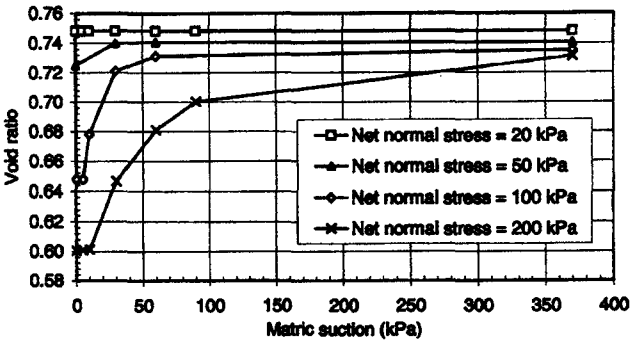

Fig. 6. Void ratio changes of soil specimens during saturation

referential volume updated at the beginning of the wetting step (Table 2). The correction for the referential volume is important in situations where large deformations occur and is approximately equivalent to the use of an Eulerian calculation. The final degrees of saturation were calculated based on the measured gravimetric water content and the final void ratio corresponding to the final step of each experiment (i.e., saturated specimen). The results in Table 3 show that larger total volume changes due to wetting were obtained for large confining stresses. As a result, a smaller volume of voids became available for the water and therefore the final water content is smaller for larger confining stresses. The final degree of saturation approached 100% for all four tests.

Table 4 summarizes the changes in both void ratio and degree of saturation versus matric suction for the four soil specimens tested. These values were calculated using the assumption that the initial loading (i.e., at a matric suction of 370 kPa) was drained in terms of the air phase and that both gravimetric water content and matric suction were constant for all soil specimens. The small decrease in total volume of the unsaturated specimen upon the initial loading caused a slight increase in the degree of saturation.

Figs. 6 and 7 present the void ratio and degree of saturation changes versus matric suction for the four collapsing specimens tested. Fig. 6 shows that the collapsing behavior is a function of both net normal stress and matric suction. A typical collapse behavior is illustrated by following a stress path of decreasing matric suction at a given net confining pressure (e.g., net confining stress of 100 kPa). Such a stress path shows that there are three distinct phases to the collapse mechanism. During the first phase, at relatively high matric suctions, the soil does not collapse and only small deformations occur in response to a decrease in matric suction. During the second phase, at intermediate matric suctions, large deformations are observed in response to a decrease in matric suction. During the third phase, at low matric suctions, there is an absence of deformations as the matric suction is reduced to zero.

Fig. 7 shows that the soil specimens present similar increases in degree of saturation, as the matric suction was reduced from a matric suction of 370 to 0 kPa, irrespective of differences in the amount of soil collapse induced by the applied net confining pressures. Soil collapse progressed in response to the gradual saturation of the soil specimen. Irrespective of the net confining pressure, soil collapse was completed before the soil specimen reached complete saturation. The influence of soil collapse is only noticed as the soil approaches complete saturation where the lower the porosity of the collapsed soil, the less is the increase in degree of saturation in response to further decreases in matric suction.

The open and metastable structure of the compacted collapsing soil is kept together by connecting bonds (e.g., clay and/or silt bridges or buttresses). The stability of such an open structure is a function of capillary action and internal microforces acting in the connecting bonds and clay aggregations. At a given net confining stress, the soil collapses in response to a reduction in matric suction and an increase in water content in the connecting bonds and clay aggregations. Both mechanisms occur during soil saturation. Results such as those presented in Figs. 6 and 7 lead to the conclusion that any explanation for the collapse of the soil structure must be related to the net normal stress. The metastable-structured soil studied can saturate without collapse of its structure under a low net confining stress [e.g., $(\sigma-u_a)=20$ kPa in Fig. 6]. In addition, a metastable-structured soil under certain ranges of net normal stress can show considerable increase in its degree of saturation without there being any collapse of the soil structure [e.g., $(\sigma-u_a)=50$ and 100 kPa in Fig. 7].

Table 4. Summary of Volume-Mass Soil Properties, Void Ratio e, and Degree of Saturation S of Collapsing Soil under Wetting Stress Path in Triaxial Tests

(u_a-u_w) (kPa)	TPT1		TPT2		TPT3		TPT4	
	e	S	e	S	e	S	e	S
370	0.7483	0.370	0.7408	0.374	0.7354	0.377	0.7314	0.379
90	0.7483	0.437	—	—	—	—	0.7003	0.423
60	0.7483	0.460	0.7406	0.445	0.7314	0.447	0.6811	0.461
30	0.7483	0.503	0.7400	0.485	0.7213	0.509	0.6468	0.525
10	0.7483	—	—	—	0.6779	0.622	0.6013	0.671
5	0.7483	—	—	—	0.6481	0.761	0.6010	0.756
0	0.7483	0.985	0.7251	0.962	0.6481	0.978	0.6007	0.956

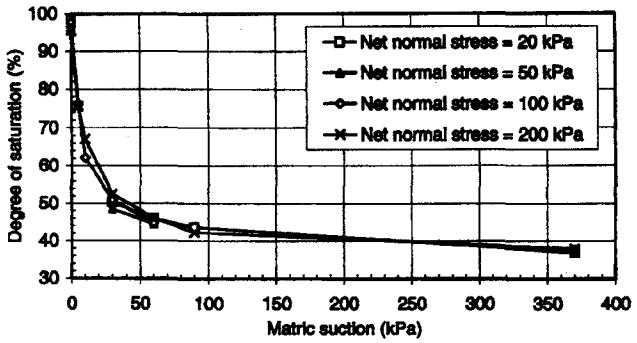

Fig. 7. Degree of saturation changes of soil specimens during saturation

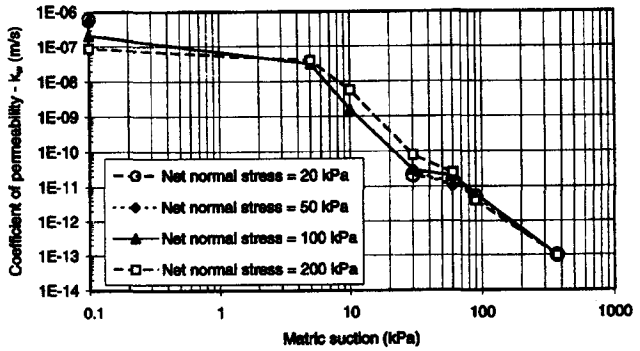

Fig. 8. Water coefficient of permeability versus matric suction of soil specimens during saturation

Coefficient of Permeability of Collapsing Soil

Table 5 presents a summary of the coefficient of permeability measurements as a function of the stress state imposed during the four collapsing tests. The coefficient of permeability obtained at zero matric suction corresponds to full saturation of the soil specimen (i.e., after applying a back pressure of 4 kPa). The coefficient of permeability for the initial condition (i.e., at matric suction of 370 kPa) was estimated from the drying (or desorption) soil-water characteristic curve (Fig. 4) using Brooks and Corey's (1964) method.

Fig. 8 presents a plot of the coefficient of permeability versus matric suction, corresponding to the four different net confining stresses. The coefficient of permeability for each soil specimen under wetting stress paths varied in a similar manner with a degree of saturation change. The small amounts of water flow made it difficult to determine the influence of gradual soil collapse on the unsaturated coefficient of permeability of the specimens. A qualitative analysis suggests that soil collapse produces localized increases (i.e., at microstructure level) in the degree of saturation. These changes affect the coefficient of permeability of the collapsing soil since the pore-size distribution of the soil structure is changed. The soil collapse might also generate internal hydraulic gradients that alter the water flow paths through the soil structure. During the wetting process with simultaneous soil collapse, there is a gradual transfer of water from the microstructure to the macrostructure in the soil specimen (Alonso et al. 1985).

Table 5. Summary of Measurements of Coefficient of Permeability (k_w) of Collapsing Soil under Wetting Stress Paths in Triaxial Permeability Tests

(u_a-u_w) (kPa)	Coefficient of permeability (values shown are to be multiplied by 10^{-9} m/s)			
	TPT1	TPT2	TPT3	TPT4
370[a]	0.0001	0.0001	0.0001	0.0001
90	0.005	—	—	0.0039
60	0.014	0.01	0.02	0.025
30	0.021	0.03	0.03	0.079
10	—	—	1.60	5.70
5	—	—	32.00	46.00
0[b]	600	540	210	90

[a]Coefficients of permeability based on characteristic drying soil-water curve using Brooks and Corey's (1964) method.

[b]Soil was saturated by using a back pressure of 4 kPa.

Fig. 8 also shows that the gradual soil collapse affects the unsaturated coefficient of permeability of the soil specimen only as zero matric suction is approached, while Fig. 9 shows a plot of the coefficient of permeability versus degree of saturation. The coinciding lines confirm that the degree of saturation has the primary influence on the coefficient of permeability and that the void ratio influence is noticeable only at low values of matric suction. Higher confining stresses produce increased collapse and therefore smaller final void ratios. A reduced value of void ratio produces lower coefficients of permeability. In summary, considering the range of stress states tested, the available results suggest that

1. The unsaturated coefficient of permeability of the collapsing soil is primarily a function of the degree of saturation. For the range of confining stresses used in the present study, the degree of saturation of the collapsing soil was primarily a function of the applied matric suction; and
2. The saturated coefficient of permeability is a function of the void ratio of the soil and consequently of the amount of collapse occurring along the wetting path. At low values of matric suction there is a transitional zone where the influence of soil collapse has a significant effect on the degree of saturation of the soil.

Modeling of Hydraulic Soil Behavior

Modeling the hydraulic properties of an unsaturated soil requires the definition of mathematical relationships between the coefficient of permeability and the stress state variables (Fredlund and

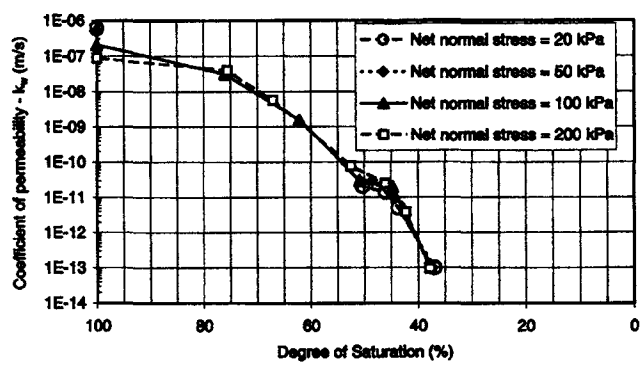

Fig. 9. Water coefficient of permeability of soil specimens versus degree of saturation

Rahardjo 1993). The definition of the soil property functions presented herein had as its main guideline the search for continuous mathematical functions that describe the available data. Selected functions were adjusted to the experimental data using best-fit regression analyses, which were performed using a Marquardt-Leveberg algorithm with the aid of the software *SigmaPlot 1.0* developed by Jandel Scientific.

Water Volume Change Behavior of Collapsing Soil

The degree of saturation constitutive surface of the collapsible soil can be described using a logistic function of four parameters. This function was found to provide an appropriate fit to the available data. Eq. (2) presents the function used:

$$S = S_0 + \frac{1 - S_0}{\left[1 + \left(\frac{(u_a - u_w)}{c}\right)^d\right]} \tag{2}$$

where $S_0 = a + b \cdot \ln(\sigma - u_a)$; $a = 0.3541$; $b = 0.003654$; $c = 7.906$; and $d = 0.9769$. Eq. (1) is a phenomenological model adequate for use in numerical analyses.

The phenomenological model for the degree of saturation presented in Eq. (2) includes the effect of changes in both the soil structure (i.e., pore size changes) and the water inflow when the collapsible soil is saturating. From a macroscopic point of view, the available data suggest that the amount of confining stress did not significantly influence the degree of saturation of the soil specimen. The low value of parameter b reflects the small effect of the soil collapse on the degree of saturation.

The constitutive function presented does not allow further considerations of the soil microstructure during saturation. The available data suggest that soil collapse produces two different and opposite effects in the saturation of the soil mass. The first effect is the reduction of the void volume in the soil mass, which increases its degree of saturation, and the second effect is the reduction in the water inflow into the micropores of the soil mass, an effect that can be enhanced by the fact that the higher the net normal stress, the more difficult it is to reach saturation in the soil specimen.

Soil specimens under net confining stress of 20 and 50 kPa appear to become saturated by using a back pressure of 4 kPa. The same back pressure appeared to produce a degree of saturation of about 97% for the soil specimen under net confining stress of 200 kPa, which may suggest that an air leakage into the soil specimen could be partly responsible for this behavior. However, the short time associated with the saturation process (i.e., when the back pressure was applied) did not appear to allow sufficient air inflow to prevent the saturation of the open-structured soil specimen.

The following additional factors can be cited to justify the difficulty in saturating the collapsing soil specimen under 200 kPa of net confining pressure:

1. Internal hydraulic gradients from the soil microstructure to the soil macrostructure caused by the soil collapse, which induces local increases in pore-water pressure in the soil microstructure (Alonso et al. 1985; Handy 1995); and
2. Air bubbles trapped in both the microstructure and macrostructure of the soil specimen when its degree of saturation is higher than 80% (Fredlund and Rahardjo 1993).

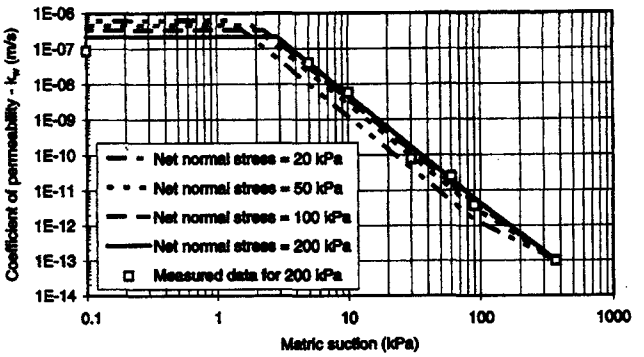

Fig. 10. Modeling of soil permeability versus matric suction relationships for collapsing soil

Coefficient of Permeability of Collapsing Soil

Figs. 8 and 9 showed that the unsaturated coefficients of permeability of the collapsing soil were not significantly affected by the net confining stress for almost the entire range of soil suction. However, when the collapsing soil specimens approach saturation, the coefficient of permeability decreases as the net confining stress is increased from 20 to 200 kPa. As previously discussed, the degree of saturation of the unsaturated soil specimens depends mainly on the applied matric suction rather than the net confining stress. At saturated conditions, the coefficient of permeability of each soil specimen depends mainly on its void ratio, which is a direct function of the net confining pressure.

The use of Brooks and Corey's (1964) equation along with a drying soil-water characteristic curve produces a close comparison between the measured coefficients of permeability and the calculated values for matric suctions higher than 5 kPa. However, the transition from the unsaturated to the saturated condition (i.e., matric suction from 5 to 0 kPa) requires some changes in the parameters for the equation to better represent the data. A modified version of Brooks and Corey's (1964) equation and the software *SigmaPlot* were used to perform a best-fit analysis of the available experimental data as a function of the stress state variables. A relationship between the saturated coefficient of permeability, k_s, and the net confining stress was previously defined and used as a constraint in the best-fit analysis. Eq. (3) presents the best-fit mathematical equation for the water coefficient of permeability of the collapsing soil.

$$k_w = k_p \left(\frac{(u_a - u_w)_b}{(u_a - u_w)}\right)^{\lambda} \tag{3}$$

where $k_w \leq k_s$; $k_s = 1.17 \times 10^{-6} - 1.8 \times 10^{-7} \cdot \ln(\sigma - u_a)$ = coefficient of permeability of the saturated soil; $k_p = -1.39 \times 10^{-7} + 6.259 \times 10^{-8} \cdot \ln(\sigma - u_a)$; $(u_a - u_w)_b = 3.0$ = soil air entry value; and $\lambda = 2.90$. Fig. 10 shows the best-fit results for different net confining stresses and also presents the available data for a net confining stress of 200 kPa to show the accuracy of the prediction model. A good fit was obtained for the entire range of matric suctions, including low values of matric suction.

Eqs. (2) and (3) have fitting capabilities proportional to the number of existing parameters. Most soil-water characteristic curve and permeability function equations found in the literature are defined by two or three parameters, providing inferior flexibility when compared to Eqs. (2) and (3). The larger number of parameters found in Eqs. (2) and (3) can be efficiently handled by commercially available nonlinear fitting software, but while the

fitting capabilities have proven successful for the data presented herein, generalizations cannot be made for all types of soil.

Eqs. (2) and (3) can be directly used in the numerical analysis of water flow in the same manner as simpler soil-water characteristic curves and permeability functions. Net normal stresses required by Eqs. (2) and (3) can be determined by solving the partial differential equations governing the static equilibrium of forces in a coupled or uncoupled manner. Pereira (1996) and Pereira and Fredlund (1999) have presented numerical models for the analysis of the coupled hydromechanical behavior of unsaturated soils using Eqs. (2) and (3). A nonlinear algorithm is required for the solution of the nonlinear partial differential equation governing the flow of water in soils. Small time steps are required to accommodate the nonlinearity of Eqs. (2) and (3). Such algorithms can be successfully combined with finite-element and finite-difference codes as shown in Pereira and Fredlund (1999).

Conclusions

The hydraulic behavior of a metastable-structured compacted soil of gneiss was studied. The testing program, which was designed to determine the volume change and permeability characteristics of the soil, comprised double-oedometer tests, pressure plate and Tempe cell tests, and consolidation and permeability tests using a triaxial permeameter. The following conclusions can be drawn from the experimental data and analysis of the results:

1. The triaxial permeameter system could be used to measure the total volume change, water content changes, and soil coefficient of permeability of a collapsing soil specimen under a constant confining pressure when following a wetting stress path. However, some problems may arise in measuring the saturated coefficient of permeability (i.e., k_s). The soil specimens being tested required back pressures to achieve complete saturation.
2. Available data suggest that the wetting-induced soil collapse produced two different and opposite effects during the saturation process while testing the unsaturated metastable-structured soil. The first effect is the reduction of the void ratio, which increases the degree of saturation of the collapsing material, and the second effect is the reduction in the water flow into the soil structure due to the increasing amount of air trapped within the microstructure of the metastable-structured soil.
3. The data obtained show that the unsaturated soil coefficient of permeability is mainly affected by the increase in degree of saturation rather than changes in the total volume of the metastable-structured soil tested. It appears that air entrapped in the soil voids may significantly reduce the soil's coefficient of permeability, which becomes dependent on the void ratio and the net mean stress as the soil approaches saturation.
4. Available theories for predicting the water coefficient of permeability that make use of the drying soil water characteristic curve seem to overestimate the permeability of a metastable-structured soil that follows a wetting-induced stress path under a given net confining pressure.
5. The fitting equations presented herein can be used in the analysis of the hydromechanical behavior of the Alka-Seltzer dams, whose failure mechanisms can be studied by considering water movement in saturated/unsaturated soils. Feasible design alternatives for the Alka-Seltzer dams can be investigated in the future using the constitutive models provided herein.

Notation

The following symbols are used in this paper:

a,b,c,d = fitting parameters;
e = void ratio;
K_0 = coefficient of earth pressure at rest;
k_p = coefficient of permeability of unsaturated soil;
k_s = coefficient of permeability of saturated soil;
k_w = complete constitutive surface for coefficient of permeability of soil;
S = degree of saturation;
u_a = pore-air pressure;
u_w = pore-water pressure;
u_a-u_w = matric suction;
$(u_a-u_w)_b$ = air-entry value;
λ = rate of decrease of coefficient of permeability versus matric suction;
σ = total confining or mean stress;
σ_v = total vertical stress;
$\sigma-u_a$ = net confining or mean stress; and
σ_v-u_a = vertical net stress.

References

Alonso, E. E., Battle, F., Gens, A., and Hight, D. W. (1985). "Special soil problems." *General Report, Proc., 9th ECSMFE*, 1087–1146.

Barden, L., McGown, A., and Collins, K. (1973). "The collapse mechanism in partially saturated soil." *Eng. Geol. (Amsterdam)*, 7(1), 49–60.

Brito, C. C., Pereira, J. H. F., Gitirana, G. F. N. Jr., and Fredlund, D. G. (2004). "Transient stability analysis of a collapsible dam using dynamic programming combined with finite element stress fields." *IXth Int. Symp. on Landslides*, 2, 1079–1084.

Brooks, R. H., and Corey, A. T. (1964). "Hydraulic properties of porous media." *Colorado State Univ. Hydrol. Paper No. 3*, Fort Collins, Colo.

Childs, E. C., and Collis-George, N. (1950). "The permeability of porous materials." *Proc., Royal Society*, 210A, 392–405.

Fredlund, D. G. (1981). "Discussion on 'Consolidation of unsaturated soils including swelling and collapse behavior,' by A. Lloret and E. E. Alonso." *Geotechnique*, 30(4), 449–477.

Fredlund, D. G., and Rahardjo, H. (1993). "Soil mechanics for unsaturated soils." Wiley, New York.

Fredlund, D. G., Xing, A., and Huang, S. (1994). "Predicting the permeability function for unsaturated soil using the soil-water characteristic curve." 31(4), 533–546.

Gardner, W. R. (1961). "Soil suction and water movement: Pore pressure and suction in soils." Butterworths, London, 137–140.

Handy, R. L. (1995). "A stress path model for collapsible loess." *Genesis and properties of collapsible soils*, E. Derbyshire, T. Dijkstra, and I. Smalley, eds., NATO, ASI-Series, Vol. 468, 33–47.

Huang, S., Barbour, S. L., and Fredlund, D. G. (1998a). "Development and verification of a coefficient of permeability function for a deformable unsaturated soil." *Can. Geotech. J.*, 35, 411–425.

Huang, S., Barbour, S. L., and Fredlund, D. G. (1998b). "Measurement of the coefficient of permeability for a deformable unsaturated soil using a triaxial permeameter." *Can. Geotech. J.*, 35, 426–432.

Lambe, T. W., and Whitman, R. V. (1979). *Soil mechanics*, Wiley, New York.

Lawton, E. C., Fragaszy, R. J., and Hardcastle, J. H. (1991). "Stress ratio

effects on collapse of compacted clayey sand." *J. Geotech. Eng.*, 117(5), 714–730.

Lloret, A., and Alonso, E. E. (1980). "Consolidation of unsaturated soils including swelling and collapse behavior." *Geotechnique*, 30(4), 449–477.

Maswoswe, J. (1985). "Stress paths for a compacted soil during collapse due to wetting." PhD dissertation, Imperial College of Science and Technology, London.

Miranda, A. N. (1988). "Behavior of small earth dams during initial filling." PhD thesis, Colorado State Univ., Fort Collins, Colo.

Mualem, Y. (1986). "Hydraulic conductivity of unsaturated soils—Prediction and formulas." *Methods of soil analysis, Part 1, Physical and mineralogical methods*, A. Klute, ed., 2nd Ed., American Society of Agronomy, Madison, Wis., 799–823.

Pereira, J. H. F. (1996). "Numerical analysis of the mechanical behavior of small collapsing earth dams during first reservoir filling." PhD thesis, Univ. of Saskatchewan, Saskatoon, Canada.

Pereira, J. H. F., and Fredlund, D. G. (1999). "Numerical analysis of the post-filling performance of small collapsing earth dams." *XIth Pan-American Conf. on Soil Mechanics and Geotechnical Engineering*, Vol. 3, 1129–1140.

Pereira, J. H. F., and Fredlund, D. G. (2000). "Volume change behavior of collapsible compacted gneiss soil." *J. Geotech. Geoenviron. Eng.*, 126(10), 907–916.

van Genuchten, M. T. (1980). "A closed-form equation of predicting the hydraulic conductivity of unsaturated soils." *Soil Sci. Soc. Am. J.*, 44, 892–898.